One-Pot Synthesis of Polypeptide–Gold Nanoconjugates for *in Vitro* Gene Transfection

Xuehai Yan,[†,*] Jenifer Blacklock,[†] Junbai Li,[‡,*] and Helmuth Möhwald[†]

[†]Max Planck Institute of Colloids and Interfaces, Am Mühlenberg 1, D-14476, Potsdam/Golm, Germany, and [‡]Beijing National Laboratory for Molecular Sciences (BNLMS), Key Lab of Colloid and Interface Sciences, Institute of Chemistry, Chinese Academy of Sciences, Beijing 100190, People's Republic of China

ABSTRACT

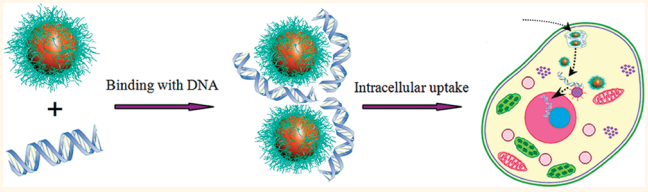

We present a general strategy to create polypeptide–gold nanoconjugates by a one-pot synthesis approach, where polypeptides act not only as capping agents but also as reductants for the formation of gold nanoparticles without the need of an additional reducing agent. The present approach is environmentally benign, facile, and flexible for the design of functional polypeptide–gold nanoconjugates. As a demonstration of as-synthesized nanoconjugates for biomedical applications, the resulting positively charged polypeptide-conjugated gold nanoparticles are applied for gene delivery. A gradual and prolonged intracellular uptake and transfection is achieved, and transfection activity is maintained for almost two weeks with no obvious cytotoxicity. The biologically based method presented in this work will provide a new alternative in creating a variety of multifunctional polypeptide–metallic nanoconjugates in a simple and straightforward manner, which will be more advantageous for their applications in biomedicine.

KEYWORDS: peptide · gold nanoparticle · one-pot synthesis · gene transfection · nanoconjugate · delivery vector

Gold nanoparticles (AuNPs) are of particular interest for widespread use in biology and medicine owing to their ease of synthesis, flexible surface modification and bioconjugation, chemical inertness, low innate cytotoxicity, and tunable optical and electronic properties (such as absorption, fluorescence, and conductivity).[1−4] One of the most promising biomedical applications of AuNPs is exploited as intracellular delivery vectors for either drugs or genes. Several attempts have been made to use AuNPs for gene delivery and transfection purposes.[5−11] For example, Klibanov and Thomas have demonstrated that polyethylenimine (PEI, 2 kDa)-conjugated AuNPs deliver plasmid DNA to COS-7 cells more efficiently as compared to PEI alone.[5] Mirkin *et al.* developed gold nanoparticle–oligonucleotide nanoconjugates as intracellular gene regulation agents for the control of protein expression in cells.[6] Amine-functionalized AuNPs developed by Rotello's group have been demonstrated to efficiently deliver DNA plasmids to mammalian cells.[7−9] Particularly the introduction of lysine-containing ligands enhances the gene transfection efficiency considerably, approximately 28-fold higher than poly lysine for *in vitro* transfections.[10] In the above-mentioned cases colloidal AuNPs have been synthesized by the classical citrate or borohydride ($NaBH_4$) reduction of chloroaurate followed by ligand exchange with suitable organic molecules or biomolecules; alternatively, they are also prepared by reducing chloroaurate in the presence of capping agents as desired. In both cases, however, the production of AuNPs has to use harsh reducing reagents such as $NaBH_4$. In addition, the ligand exchange strategy used in order to introduce biologically functionalized molecules more or less suffers from particle aggregation and incomplete exchange of ligands, which is unacceptable for biomedical applications. It thus remains a great challenge to directly synthesize metallic nanoparticles including AuNPs using only biomolecules in a simple and straightforward manner. These biomolecule-conjugated AuNPs will no doubt be more advantageous for biomedical applications including drug and gene delivery.

Herein, we report that one-pot-synthesized polypeptide-conjugated AuNPs (Figure 1A) are ideal for gene delivery and efficient transfection activity. In our strategy, positively charged polypeptides (*e.g.*, poly-L-lysine, PLL) were used to serve not only as capping agents but also as reductants without the need for an external reducing agent. Functions and properties of the polypeptide are determined by

* Address correspondence to xuehai.yan@mpikg.mpg.de; jbli@iccas.ac.cn.

Received for review August 2, 2011 and accepted November 28, 2011.

Published online December 05, 2011
10.1021/nn202939s

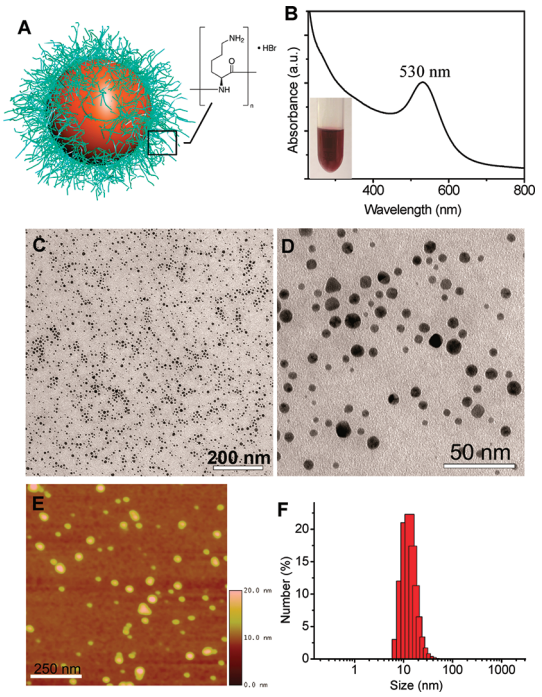

Figure 1. (A) Scheme of polypeptide-conjugated gold nanoparticles synthesized using the one-step strategy. (B) UV−vis absorption spectrum of MPL-conjugated AuNPs and photograph of an aqueous solution containing AuNPs (inset). (C,D) TEM micrographs of AuNPs at low (left) and higher (right) magnification. (E) AFM height image of AuNPs. (F) DLS size-distribution diagrams of AuNPs.

the type and sequence of its constituent amino acids.[12−15] In this regard, the present strategy of fabricating AuNPs using PLL can be readily expanded to other polypeptides containing amino acids with reduction capability,[16−18] indicating a general suitability for synthesis of AuNPs coated with various functional polypeptides. To verify the versatility (or feasibility) of polypeptide-conjugated AuNPs for biomedical applications, we studied the gene delivery and transfection activity *in vitro* using PLL-conjugated AuNPs. We find that positively charged polypeptide-conjugated AuNPs effectively bind and condense DNA via electrostatic interactions, serving as efficient DNA delivery systems. Cell transfection studies show that polypeptide−AuNP nanoconjugates apparently enhance the transfection activity at a relatively low dosage (*e.g.*, 2.5 $\mu g \cdot mL^{-1}$) without compromising cell viability. The polypeptide−gold nanoconjugates synthesized by a one-step strategy provide a new means to engineer and develop delivery vectors for both drugs and genes.

RESULTS AND DISCUSSION

PLL with different molecular weight was used to investigate the ability to reduce chloroauric acid ($HAuCl_4$) and stabilize the AuNPs formed. When an aliquot of aqueous $HAuCl_4$ solution was added to the phosphate buffered saline (PBS) solution of PLL with low molecular weight (LPL, 500−2000), a reddish-colored

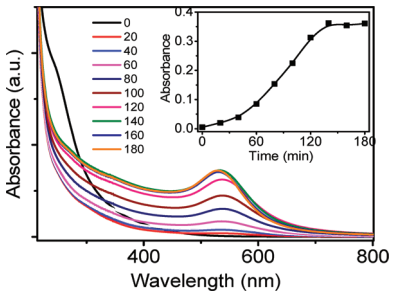

Figure 2. UV−vis spectra obtained as a function of time (time interval = 20 min) after adding $HAuCl_4$ solution to an aqueous MPL solution at 65 °C. The inset shows a plot of the absorption at the maximum *vs* the time.

solution was formed within 12 h at room temperature. However, the solution color gradually turned to blue and subsequently black and eventually resulted in the agglomeration and precipitation of nanoparticles upon standing within 2 days. Transmission electron microscopy (TEM) images confirm the presence of nanoparticle aggregates (Figure S1). This observation indicates that LPL is potent in reducing $HAuCl_4$, but fails to stabilize the nanoparticles formed. To obtain water-stabilized and well-dispersed gold nanoparticles, we thus selected PLL with higher molecular weight to reduce $HAuCl_4$. This is based on the fact that more charges of PLL are available for higher molecular weight, benefiting the stabilization of AuNPs. In this case, however, we find that elevated temperatures are essential for triggering the reaction due to the stronger binding interaction between PLL and $HAuCl_4$. The reddish-colored solution containing AuNPs (inset in Figure 1B) obtained as a mixed solution comprising $HAuCl_4$ (1 mM) and PLL (1 $mg \cdot mL^{-1}$) with medium (MPL, 15−30 kDa) or high (HPL, 30−70 kDa) molecular weight was incubated for 3 h in a 65 °C water bath. The reddish color is ascribed to the surface plasmon resonance (SPR) of AuNPs. The UV−vis spectrum (Figure 1B) of MPL-conjugated AuNPs (MPL-Au) exhibits a SPR band at 530 nm, further confirming the formation of AuNPs by PLL. The TEM images (Figure 1C,D) show well-dispersed AuNPs having an average diameter of 15 nm. The AFM image in Figure 1E also indicates well-dispersed spherical AuNPs. The size of MPL-conjugated AuNPs determined by dynamic light scattering (DLS) shows a relatively narrow distribution of 15 ± 7 nm (Figure 1F), in agreement with the TEM analysis. Zeta potential measurements reveal that MPL-conjugated AuNPs have a positive surface charge (~18 mV), suggesting the successful capping of PLL onto the surface of AuNPs.

To gain further insight into AuNP formation by polypeptides, we collected the time-dependent UV−vis spectra of mixed solutions of $HAuCl_4$ (1 mM) and MPL (1 $mg \cdot mL^{-1}$) at a constant temperature of 65 °C (Figure 2). Visually, the yellow color of the mixed solution faded gradually and changed to colorless in a few minutes and eventually to cardinal red when the sample was kept at 65 °C for 3 h. The corresponding UV−vis

spectra reflect the time development of a SPR band with a maximum initially at 537 nm and finally at 530 nm. In comparison with the SPR peak (530 nm) of AuNPs formed ultimately, the slight blue-shift in the process of particle growth may be due to the dynamic decomposition and recombination of AuNPs during the reaction so as to reach equilibrium.[19] A plot of the respective SPR peak *versus* time is given to further dissect the growth kinetics of AuNPs. Apparently, the rate of particle formation is relatively slow at the beginning and increases almost linearly with time until reaching equilibrium (inset in Figure 2). This result indicates that once gold nuclei are formed, albeit slowly, they lead to fast growth of the corresponding nanoparticles. The reduction of gold ions by PLL is likely based on the mechanism of metal ion induced oxidation of amine to nitrite.[19] The amino groups at the side chains of PLL are assumed to be responsible for the electron donation, analogous to the case of amine-containing molecules in reducing gold salts.[21,22] Taken together, these results imply that PLL with appropriate molecular weight can act as both reducing and capping agent for synthesizing AuNPs. The spontaneous formation of AuNPs is attributed to the direct redox reaction between amino groups of PLL and gold salt ions ($AuCl_4^{-1}$). The stabilization of the resulting AuNPs is guaranteed by a combination of steric and electrostatic interactions of charged polypeptides.

To verify the general suitability of the present strategy, the copolypeptide, poly(Phe, Lys) (PPL), was employed for the synthesis of AuNPs. As 5 μL of $HAuCl_4$ (0.1 M) was added to a PBS solution of PPL with a final concentration of 1 mg·mL^{-1} and incubated for 3 h at a constant temperature of 65 °C, likewise, it is observed that the solution color gradually turned red over time, indicating the occurrence of AuNPs. This is further evidenced by the TEM observation, revealing AuNPs with an average size of 10 nm (Figure S2).

PLL-conjugated AuNPs (MPL-Au or HPL-Au) having a positive charge show a potential to condense negatively charged DNA. To validate the binding between both, a standard ethidium bromide (EtBr)-DNA fluorescence quenching exclusion assay was carried out.[23,24] EtBr is an intercalating agent commonly used as a fluorescent tag. Upon attachment to DNA, the fluorescence intensifies almost 20-fold more than intercalating DNA with respect to the free state in solution. EtBr can be extruded as DNA binds with delivery vectors and quenches in solution. This is applicable to determine whether PLL-conjugated AuNPs bind DNA. The EtBr displacement assay shows the fluorescence intensity as a function of charge ratios of MPL to DNA (Figure3). The decay of the EtBr-fluorescence intensity with the increase of the MPL-Au proportion indicates complexation between DNA and positively charged MPL-Au nanoparticles.

On the basis of the above fluorescence quenching exclusion assay, the charge ratio of 4:1 of PLL to DNA

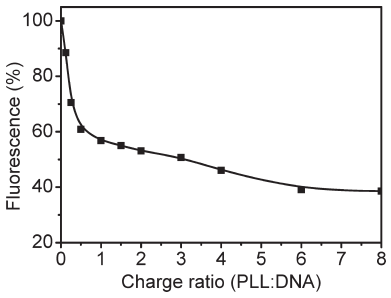

Figure 3. EtBr displacement assay of PLL-conjugated AuNPs binding DNA, showing the fluorescence intensity as a function of PLL/DNA charge ratio.

was selected to prepare PLL-Au-DNA complexes, which are formed via electrostatic attraction between the phosphate groups of DNA and amino groups of the PLL components (Figure 4). DLS shows that the ternary complexes (MPL-Au-DNA or HPL-Au-DNA) have a narrow size distribution with an average diameter of 1.2 and 1.5 μm, respectively (Figure S3A,B). The zeta potential is around 12 mV for MPL-Au-DNA and 16 mV for HPL-Au-DNA complexes, respectively. Compared to the individual PLL-conjugated AuNPs, the increase of size and the corresponding decrease of zeta potential indicate the condensation between PLL-conjugated AuNPs and DNA. In addition, it is clear that the increase of the PLL molecular weight leads to an increase of the zeta potential, which more likely facilitates the intracellular uptake and thus enhances the transfection efficiency.

The stability of PLL−gold nanoconjugates was also assessed in the presence of biological media. As the complexes of nanoconjugates (MPL-Au or HPL-Au) and DNA were added to both Dulbecco's modified Eagle's medium (DMEM) and bovine serum albumin (BSA), we found that they are stable over 2 weeks (Figure S4). In the case of DMEM only a slight change in size was initially observed, whereas the particle size increase when BSA was added accounts for an increase of 100 nm due to protein adsorption on the ternary complexes via electrostatic attraction. As a control experiment, we also inspected the size change of MPL-DNA or HPL-DNA complexes under the same conditions (Figure S4). A similar phenomenon was observed indicating the stability of the complexes in biological media. Namely, the components of the biological media do not break the complexes formed between nanoconjugates or individual PLL and DNA. The results indicate that the polypeptides are strongly bound to AuNPs to form the conjugates, and no displacement occurs in the biological medium. Such stability is favorable for their application in gene or drug delivery.

Transfection experiments using the reporter gene, green fluorescent protein plasmid DNA (gfpDNA), were performed with NIH-3T3 fibroblast cells. Cells treated with MPL-Au-DNA (Figure 5) or HPL-Au-DNA particles

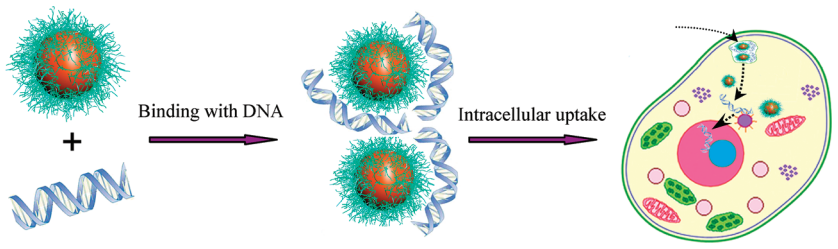

Figure 4. Schematic illustration of positively charged polypeptide-conjugated AuNPs binding with DNA for intercellular delivery.

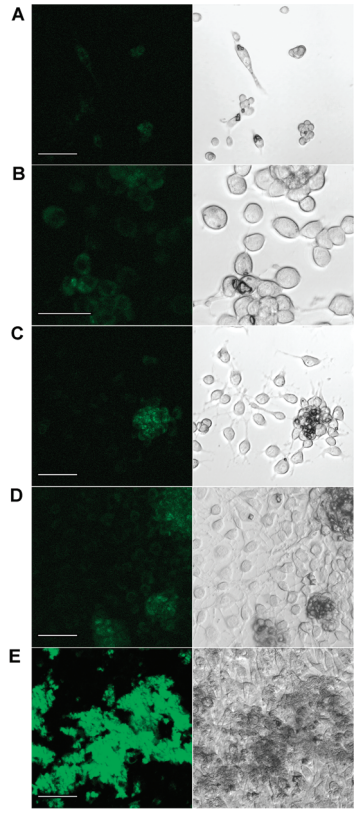

Figure 5. Confocal images of transfected cells treated with MPL-Au-DNA complexes for different times: (A) 2 days, (B) 3 days, (C) 4 days, (D) 6 days, and (E) 10 days. Left: confocal fluorescence. Right: bright-field images. Scale bar is 50 μm.

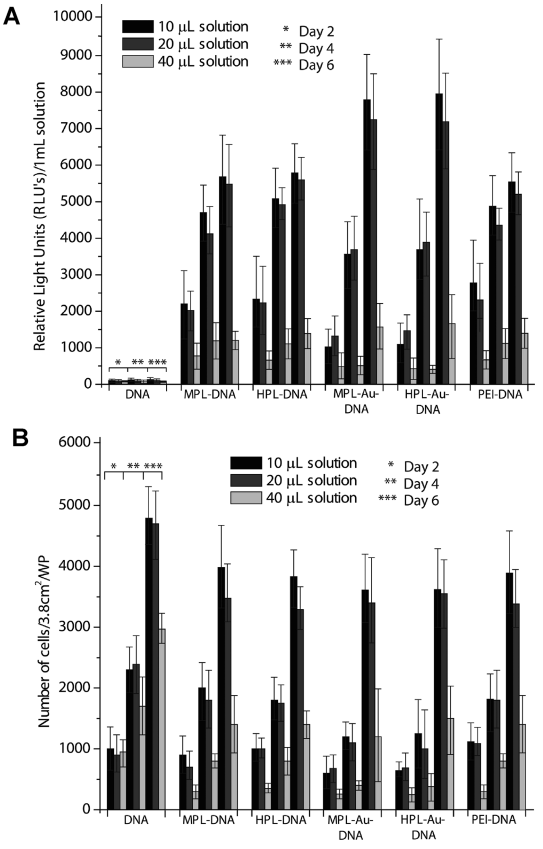

Figure 6. Transfection activity (A) and cytotoxicity (B) studies of PLL-conjugated AuNPs for different incubation times and particle dosages.

(Figure S5) over 2 days are found to be only slightly transfected (Figure 5A). Significantly, most cells preferentially grew around the clusters of ternary complexes, which were clearly observed after incubation for 3 or 4 days. This probably originates from the interaction between positively charged clusters and the cellular plasma membrane that carries a negative charge.[10] As the cells proliferate, they are attracted to the clusters and grow around and on top of them. Furthermore, it is found that increased amounts of cells fluoresce with increasing incubation time, indicating increased levels of transfection activity. The transfection activity of ternary complexes is quantified in comparison with naked DNA (DNA that is not complexed) and individual MPL-DNA and HPL-DNA complexes and commercial transfection reagent PEI-DNA complexes (Figure 6A). The results show that there is increased transfection activity when a low concentration of complexes (2.5 or 5 $\mu g \cdot mL^{-1}$) is added to the cell culture compared to a higher dosage ($10\,\mu g \cdot mL^{-1}$). In general, MPL-DNA, HPL-DNA, and PEI-DNA complexes have increased transfection activity within the first few days compared to MPL-Au-DNA and HPL-Au-DNA complexes, which are found to have prolonged transfection activity over 10 days. This is most likely due to the increased number of clusters of ternary complexes in cell culture medium preventing cell growth within the first few days. Nevertheless, it was found that within a week the cells are able to spontaneously break apart the clusters and begin

proliferating and taking up the DNA and thus maintain a longer tranfection activity. To gain further insight into the prolonged transfection activity, we monitored the cells transfected for 10 days (Figure 5E and Figure S5B). It was found that the cells spread over the whole well plate and a lot of green fluorescent proteins were produced, indicating more cells were transfected. The surprising prolonged transfection activity is ascribed to the relatively larger clusters (or agglomerates) formed between PLL-Au nanoconjugates and DNA with respect to the PLL-DNA or PEI-DNA complexes. On the one hand, the big clusters inhibit cell growth and proliferation at the beginning. On the other hand, with the cell proliferation, more and more small particles are accessible due to disassembly of the big clusters into smaller complexes through cellular enzymatic degradation of the PLL. This process offers the sustained release of PLL-Au-DNA complexes, thus leading to gradual cellular internalization of DNA. Both of these factors contribute to the prolonged transfection via the use of polypeptide-conjugated AuNPs. This observation implies that the polypeptide–gold nanoconjugates are promising for gene transfection, particularly in the aspect of prolonging the transfection activity. As for the uptake mechanism of the complexes, it is assumed that endocytosis is responsible for the intracellular uptake of the complexes. There have been relationships found between particle size and the endocytotic mechanism.[25,26] It has been found that the pathway can be shifted to lipid-raft-mediated (or caveolae-mediated, a subtype of lipid-raft-mediated uptake) internalization for micrometer-sized particles such as the polystyrene beads ($\sim$1 μm)[25] and the polyelectrolyte microcapsules ($\sim$4 μm).[27] As illustrated above, the size distribution of the PLL-Au-DNA complexes is approximately 1–2 μm; thus it can be conjectured that these complexes are taken up through an endocytotic mechanism.

Cytotoxicity of polypeptide-conjugated AuNPs as potential delivery vectors was evaluated using a standard WST-1 reagent. Proliferation was studied using a lactate dehydrogenase (LDH) assay (Figure 6B). It was found that cell proliferation is strongly dependent on the density of the complexes added to the cell culture. When concentrations above 5 $\mu g \cdot mL^{-1}$ were added to the cell culture, cells sense that there is less room to proliferate, leading to decreased levels of cell growth with increased toxicity levels. Additionally, cells appear to grow better within the first few days with complexes that do not contain AuNPs. This is most likely due to the increased size and clustering of the complexes containing AuNPs compared to those without AuNPs. Viability studies show that cellular toxicity is directly related to the concentration of complexes in cell culture as well as their size and degree of clustering. It is found that with increased MPL-Au-DNA and HPL-Au-DNA concentration from 2.5 $\mu g \cdot cm^{-2}$ to 15.0 $\mu g \cdot cm^{-2}$, the toxicity increases 2-fold. It also appears that with increased concentration of the complexes, aggregation also increases, leading to higher toxicity levels. When looking at the complexes with AuNPs, it is found that MPL-Au-DNA and HPL-Au-DNA have increased toxicity levels over the first three days compared to MPL-DNA, HPL-DNA, and PEI-DNA complexes. This is likely due to the increased size and clustering of the complexes with AuNPs in the first few days. The assumption is also evidenced by DLS results, which show larger MPL-Au-DNA and HPL-Au-DNA complexes with respect to MPL-DNA and HPL-DNA complexes (Figure S3). However, when the cells begin to proliferate, they break apart the clusters, and after day 3 the toxicity is decreased and is similar to the toxicity levels of the complexes without AuNPs.

Normally, clustering or bigger agglomerates of delivery vectors are unfavorable for gene delivery, commonly causing severe cell toxicity. In our case, however, the clusters do not lead to high levels of cell toxicity, even though there are many clusters present. This phenomenon is surprising, especially the decrease of cytotoxicity and apparently enhanced transfection activity over several days. This implies that the delivery vectors we have developed are efficient for achieving intracellular delivery, release, and transfection of genes (Figure 4). The fact that the bigger condensed complex particles may be much more resistant to enzymatic degradation of DNA suggests further application *in vivo*. Particularly, the transfection is effectively prolonged through sustained cellular uptake of polypeptide-AuNP-DNA complexes, rendering the polypeptide-conjugated AuNPs as promising candidates for introducing DNA into cells.

CONCLUSION

In summary, we have developed a facile, one-step strategy to synthesize water-stable gold nanoparticles capped with positively charged polypeptides. This approach can be readily extended to a broad variety of naturally occurring polypeptides and artificially synthesized copolypeptides containing amino acids with reduction capability. On account of the flexible incorporation of functions, relatively simple components, and natural biocompatibility of polypeptides, the gold nanoparticles formed by such a biologically based protocol will be versatile for biomedical applications. In this regard, positively charged polypeptide-conjugated gold nanoparticles have been demonstrated to be effective gene delivery vectors. A gradual and prolonged intracellular uptake and transfection is achieved, and transfection activity is maintained for almost two weeks without compromising the cell viability. Although these multiple complex systems have not yet been optimized for maximum efficacy, the ability to flexibly control polypeptide

components and motifs capped on the nanoparticle surface will allow us to engineer distinctive cooperative properties including, for example, specific recognition and enhanced target binding. Such functional polypeptide–gold nanoconjugates will provide a potential alternative for delivery of drugs and genes.

METHODS

Materials. Poly-L-lysine hydrobromide (PLL, M_w 500–2000, 15–30 kDa, and 30–70 kDa), branched polyethylenimine (PEI, M_w 25 kDa), and poly(Phe, Lys) 1:1 hydrobromide (PPL, M_w 20–50 kDa) were purchased from Sigma-Aldrich. Chlorauric acid ($HAuCl_4$) is a product of Alfa Aesar. High-expression green fluorescent protein plasmid (gfpDNA, 6732bp) was purchased from aldevron. All other chemicals were purchased from Sigma-Aldrich.

Synthesis and Characterization of Polypeptide-Conjugated AuNPs. A typical protocol was as follows: Gold nanoparticles were synthesized by adding 10 μL of $HAuCl_4$ (0.1 M) to a PBS solution of PLL with a final concentration of 1 mg·mL^{-1}. Subsequently, the mixture was incubated for 3 h within a 65 °C water bath. The formation of gold nanoparticles was monitored by UV–vis spectroscopy with a UV–vis spectrophotometer (Varian Cary 500 or 1000). Size distribution and zeta potential of AuNPs were recorded using a Zetasizer (Malvern Instrument). TEM images of AuNPs were obtained with a Zeiss EM 912 Omega transmission electron microscope operated at 120 kV, where samples were carefully placed onto the carbon-coated copper grids. AFM images were obtained with a Nanoscope IIIa (Digital Instruments, Veeco Metrology Group) in tapping mode under ambient conditions.

DNA Binding Affinities. DNA binding studies were accomplished by a standard ethidium bromide (EtBr)-DNA fluorescence quenching exclusion assay. A series of MPL-Au-DNA complexes were obtained at different charge ratios of PLL to DNA (from 0.25:1, 0.5:1, 1:1, to 8:1, as shown in Figure 3) by a mixture of MPL-AuNPs and DNA. Briefly, a certain amount of MPL-AuNPs (1 mg·mL^{-1} based on the concentration of MPL) was diluted by PBS solution. Afterward, a 0.2 mL PBS solution of DNA (100 μg·mL^{-1}, stained with EtBr in advance) was added to the above solution. The final volume of solution is 2 mL, suitable for the fluorescence measurement. The EtBr-DNA fluorescence quenching exclusion assay was carried out using a Fluoromax-4 spectrofluorometer (Horiba Jobin Yvon) with a 1.0 cm quartz cuvette. Each complex was incubated for 20 min at room temperature prior to the measurement.

Stability of PLL–Gold Nanoconjugates. Stability of the PLL-Au-DNA complexes was determined by placing the complexes in a solution of 10 mM BSA and DMEM over several days. Time points were taken with DLS to measure size and zeta potential of the particles in order to better interpret their stability over time.

Cell Viability and Transfection Studies. For all samples used for gene transfection and cell viability, 20 μL of 1 mg·mL^{-1} DNA solution was added to 500 μL of PLL-Au nanoparticle solution (0.2 mg·mL^{-1}), and the complexes were vortexed at medium speed for 5 min and left to sit for 20 min before addition to the cell culture. Then 10, 20, and 40 μL of this solution were added to different well plates to investigate various particle densities with regard to cell viability and transfection. The amount of DNA used in naked DNA control and positive control experiments was the same as above. NIH-3T3 cells were grown to 80% confluence, trypsinized, washed with PBS (pH 7.0–7.2), and resuspended in Dulbecco's modified Eagle's medium. Then, 10 000 cells were placed in a 12-well plate and incubated in 5% CO_2 at 37 °C for 1 h. All particles were added to the well plate in DMEM before the cells were added to the well plates, unless noted otherwise. Cell culture medium was replaced every day by carefully washing the well plates with PBS and transferring new DMEM medium into the well plates. Cells were imaged daily by optical and fluorescence microscopy. The images were acquired at 37 °C using excitation/emission filters of 435–485 nm. An assay with the cell proliferation reagent lactate dehydrogenase was carried out in parallel with the WST-1 reagent for cell viability studies. LDH was used to quantify cell attachment and proliferation using a commercial CytoTox 96 nonradioactive cytotoxicity assay kit (Promega). At different time points, the cells were washed with PBS and lysed by three freeze–thaw cycles. Then 50 μL of the stop solution was added to each sample, and the absorbance was measured at 490 nm. A calibration curve (cell number *vs* LDH content) was constructed using a known number of cells. The results are expressed as mean number of cells per cm^2 of the well plate ± SD (standard deviation) obtained from four samples. The WST-1 procedure was carried out using 2 mL of fresh serum-free DMEM without phenol red. A 200 μL amount of the WST-1 reagent was added to each of the well plates and incubated for an additional 4 h at 37 °C under 5% CO_2 in a humidified incubator. Controls were used with the absence of cell attachment to the well plates. The absorbance was measured in an ELISA microplate reader (Bio-Rad) at 450/650 nm, and the percent cytotoxicity was calculated by subtracting the background from the sample.

Acknowledgment. X.Y. acknowledges support for a research fellowship from the Alexander von Humboldt Foundation. X.Y. greatly thanks H. Runge and R. Pitschke for TEM measurements and A. Heilig for kind assistance in AFM measurement. We acknowledge the biomaterials department in the MPIKG for the help of cell incubation. The authors acknowledge the financial support of this research by the German Max-Planck Society, the National Basic Research Program of China (973 Program) 2009CB30101, and the Chinese Academy of Sciences.

Supporting Information Available: TEM images of AuNPs synthesized using LPL or poly(Phe, Lys); DLS size-distribution diagrams of PLL-Au-DNA and PLL-DNA complexes; study of the stability of PLL–gold nanoconjugates; confocal images of cells treated with HPL-Au-DNA complexes; and transfection study with seeding cells first in the well plate. This material is available free of charge via the Internet at http://pubs.acs.org.

REFERENCES AND NOTES

1. Boisselier, E.; Astruc, D. Gold Nanoparticles in Nanomedicine: Preparations, Imaging, Diagnostics, Therapies and Toxicity. *Chem. Soc. Rev.* **2009**, *38*, 1759–1782.
2. Ghosh, P.; Han, G.; De, M.; Kim, C. H.; Rotello, V. M. Gold Nanoparticles in Delivery Applications. *Adv. Drug Delivery Rev.* **2008**, *60*, 1307–1315.
3. Sperling, R. A.; Rivera, P.; Gil, Zhang, F.; Zanella, M.; Parak, W. J. Biological Applications of Gold Nanoparticles. *Chem. Soc. Rev.* **2008**, *37*, 1896–1908.
4. Giljohann, D. A.; Seferos, D. S.; Daniel, W. L.; Massich, M. D.; Patel, P. C.; Mirkin, C. A. Gold Nanoparticles for Biology and Medicine. *Angew. Chem., Int. Ed.* **2010**, *49*, 3280–3294.
5. Thomas, M.; Klibanov, A. M. Enhancing Polyethylenimine's Delivery of Plasmid DNA into Mammalian Cells. *Proc. Natl. Acad. Sci. U. S. A.* **2003**, *100*, 9138–9143.
6. Rosi, N. L.; Giljohann, D. A.; Thaxon, C. S.; Lytton-Jean, A. K. R.; Han, M. S.; Mirkin, C. A. Oligonucleotide-Modified Gold Nanoparticles for Intracellular Gene Regulation. *Science* **2006**, *312*, 1027–1030.
7. Han, G.; Martin, C. T.; Rotello, V. M. Stability of Gold Nanoparticle-Bound DNA toward Biological, Physical, and Chemical Agents. *Chem. Biol. Drug Des.* **2006**, *67*, 78–82.
8. Sandhu, K. K.; McIntosh, M. M.; Smard, J. M.; Smith, S. W.; Rotello, V. M. Gold Nanoparticle-Mediated Transfection of Mammalian Cells. *Bioconjugate Chem.* **2002**, *13*, 3–6.
9. Han, G.; Chari, N. S.; Verma, A.; Hong, R.; Martin, C. T.; Rotello, V. M. Controlled Recovery of the Transcription of

Nanoparticle-Bound DNA by Intracellular Concentrations of Glutathione. *Bioconjugate Chem.* **2005**, *16*, 1356–1359.
10. Ghosh, P. S.; Kim, C. K.; Han, G.; Forbes, N. S.; Rotello, V. M. Efficient Gene Delivery Vectors by Tuning the Surface Charge Density of Amino Acid-Functionalized Gold Nanoparticles. *ACS Nano* **2008**, *2*, 2213–2218.
11. Lee, S. K.; Han, M. S.; Asokan, S.; Tung, C.-H. Effective Gene Silencing by Multilayered siRNA-Coated Gold Nanoparticles. *Small* **2011**, *7*, 364–370.
12. Yan, X. H.; Zhu, P. L.; Li, J. B. Self-Assembly and Application of Diphenylalanine-Based Nanostructures. *Chem. Soc. Rev.* **2010**, *39*, 1877–1890.
13. Yan, X. H; Zhu, P. L.; Fei, J. B.; Li, J. B. Self-Assembly of Peptide-Inorganic Hybrid Spheres for Adaptive Encapsulation of Guests. *Adv. Mater.* **2010**, *22*, 1283–1287.
14. Deming, T. J. Synthetic Polypeptides for Biomedical Applications. *Prog. Polym. Sci.* **2007**, *32*, 858–875.
15. Yan, X. H.; Li, J. B.; Möhwald, H. Self-Assembly of Hexagonal Peptide Microtubes and Their Optical Waveguiding. *Adv. Mater.* **2011**, *23*, 2796–2801.
16. Tan, N.; Yang Lee, J.; Wang, D. I. C. Uncovering the Design Rules for Peptide Synthesis of Metal Nanoparticles. *J. Am. Chem. Soc.* **2010**, *132*, 5677–5686.
17. Slocik, J. M.; Stone, M. O.; Naik, R. R. Synthesis of Gold Nanoparticles Using Multifunctional Peptides. *Small* **2005**, *1*, 1048–1052.
18. Tkachenko, A. G.; Xie, H.; Coleman, D.; Glomm, W.; Ryan, J.; Anderson, M. F.; Franzen, S.; Feldheim, D. L. Multifunctional Gold Nanoparticle-Peptide Complexes for Nuclear Targeting. *J. Am. Chem. Soc.* **2003**, *125*, 4700–4701.
19. Huang, H.; Yang, X. Synthesis of Chitosan-Stabilized Gold Nanoparticles in the Absence/Presence of Tripolyphosphate. *Biomacromolecules* **2004**, *5*, 2340–2346.
20. Capdevielle, P.; Lavigne, A.; Sparfel, D.; Lafont-Baranne, J.; Cuong, N. K.; Maumy, M. Mechanism of Primary Aliphatic-Amines Oxidation to Nitriles by the Cuprous Chloride-Dioxygen-Pyridine System. *Tetrahedron Lett.* **1990**, *31*, 3305–3308.
21. Chen, C. C.; Hsu, C. H.; Kuo, P. L. Effects of Alkylated Polyethylenimines on the Formation of Gold Nanoplates. *Langmuir* **2007**, *23*, 6801–6806.
22. Sun, X.; Dong, S.; Wang, E. High-Yield Synthesis of Large Single-Crystalline Gold Nanoplates through a Polyamine Process. *Langmuir* **2005**, *21*, 4710–4712.
23. Wang, K. W.; Yan, X. H.; Cui, Y.; He, Q.; Li, J. B. Synthesis and in vitro Behavior of Multivalent Cationic Lipopeptide for DNA Delivery and Release in Hela Cells. *Bioconjugate Chem.* **2007**, *18*, 1735–1738.
24. Prata, C. A. H.; Zhao, Y. X.; Barthelemy, P.; Li, Y.; Luo, D.; McIntosh, T. J.; Lee, S. J.; Grinstaff, M. W. Charge-Reversal Amphiphiles for Gene Delivery. *J. Am. Chem. Soc.* **2004**, *126*, 12196–12197.
25. Rejman, J.; Oberle, V.; Zuhorn, I. S.; Hoekstra, D. Size-Dependent Internalization of Particles via the Pathways of Clathrinand Caveolae-Mediated Endocytosis. *Biochem. J.* **2004**, *377*, 159–169.
26. Chithrani, B. D.; Chan, W. C. W. Elucidating the Mechanism of Cellular Uptake and Removal of Protein-Coated Gold Nanoparticles of Different Sizes and Shapes. *Nano Lett.* **2007**, *7*, 1542–1550.
27. De Geest, B. G.; Vandenbroucke, R. E.; Guenther, A. M.; Sukhorukov, G. B.; Hennink, W. E.; Sanders, N. N.; Demeester, J.; De Smedt, S. C. Intracellularly Degradable Polyelectrolyte Microcapsules. *Adv. Mater.* **2006**, *18*, 1005–1009.